JOURNAL
OF THE AMERICAN CHEMICAL SOCIETY

VOLUME 99, NUMBER 12 JUNE 8, 1977

Bond Length Changes Resulting from Halogen Substitution on Three-Membered Rings

Carol A. Deakyne, Leland C. Allen,* and Norman C. Craig[1a]

Contribution from the Department of Chemistry, Princeton University, Princeton, New Jersey 08540. *Received September 13, 1976*

Abstract: Halogen substituents are known to alter the bond lengths in a cyclopropane ring. Orbital composition, atomic charges and overlap populations, orbital energy correlation diagrams, and charge density difference plots obtained from ab initio wave functions are investigated in determining the origin of the observed substituent effects. The experimentally determined bond length changes in 1,1-difluorocyclopropane and 3,3-difluorocyclopropene are explained, bond length changes for 1,1,2,2-tetrafluorocyclopropane, fluorocyclopropane, and *cis*-1,2-difluorocyclopropane are predicted, and a conflict between experimental results on 1,1-dichlorocyclopropane is resolved. The method employed for the cyclopropane ring can be extended to cyclopropene and the geometry of 3,3-difluorocyclopropene rationalized. A simple additivity rule is demonstrated whereby bond length changes produced by successive halogen substitution can be obtained by superposition; e.g., knowledge of the bond length changes in 1,1-difluorocyclopropane can be used to predict bond length changes in *cis*-1,2,3-trifluorocyclopropane. It is found that Mulliken overlap populations lead to incorrect predictions for bond length changes in almost all molecules treated and an explanation of when and why this comes about is given. Orbital energy correlation diagrams avoid the problems inherent to overlap populations, but for larger systems (e.g., 1,1,2,2-tetrafluorocyclopropane) their intricacy makes them impractical. Charge density difference plots, analyzed in terms of Hellmann-Feynman theorem force vectors, provide a direct and easy to visualize method applicable to all molecules considered. In the continuing effort to evaluate the extensively employed semiempirical methods a set of parallel calculations was carried out for 1,1-difluorocyclopropane. The same general conclusions are obtained from the semiempirical and ab initio wave functions, although some molecular properties differ.

I. Introduction

Substitution on a cyclopropane ring is known to affect the geometry of the ring.[1-19] For electronegative groups, the ring bonds adjacent to the substituent(s) shorten and the ring bond opposite the substituent(s) lengthens relative to the bond distances in cyclopropane (I).[13-16,18,19] In this paper, the following fluoro-substituted cyclopropanes were considered in detail and ab initio wave functions determined for each: 1,1-difluorocyclopropane (II), 1,1,2,2-tetrafluorocyclopropane (III), fluorocyclopropane (IV), *cis*-1,2-difluorocyclopropane (V), and *cis*-1,2,3-trifluorocyclopropane (VI).

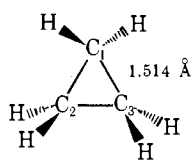

I

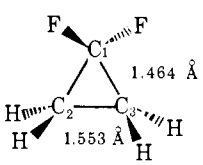

II

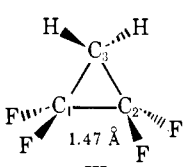

III

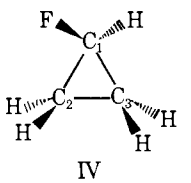

IV

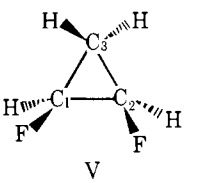

V

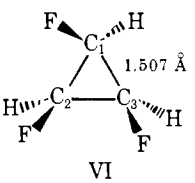

VI

Using cyclopropane (I) as the reference molecule, we compare its orbital compositions, orbital energy correlation diagrams, overlap populations, and charge distribution with the substituted molecules (the cyclopropane ring geometry is retained in the fluoronated species II-VI). The experimentally determined geometries in 1,1-difluorocyclopropane (II)[15] and 3,3-difluorocyclopropene[23] are rationalized, bond length changes for fluorocyclopropane (IV) are predicted, and a resolution for the conflicting experimental data in the literature for 1,1-dichlorocyclopropane[17,18] is suggested.

The methodological approach adopted in this paper is to exploit the better known and more widely used analysis schemes (generally those requiring less accurate wavefunctions) as fully as possible before considering other methods. Thus we are able to gain a great deal of knowledge about bond length changes in the molecules of interest from substituent induced changes in orbital compositions and overlap populations. However, because the molecules treated are strained, overlap population predictions are incorrect for many bonds. Orbital energy correlation diagrams are then used to give the correct weighting to substituent interactions. For the more heavily substituted rings orbital energy correlation diagrams as well as overlap populations lose their capabilities and charge density difference plots are the appropriate technique. These maps are interpreted by assigning forces (defined by the Hellmann-Feynman theorem) to the charge gains and losses

Table I. Geometrical Parameters

Molecule	R_{CC}, Å	R_{CF}, Å	R_{CH}, Å	∠CCC, deg	∠FCF, deg	∠HCF, deg	∠HCH, deg
I	1.514		1.080	60.0			116.0
II	1.514	1.355	1.080	60.0	108.3		116.0
III	1.514	1.355	1.080	60.0	108.3		116.0
IV	1.514	1.354	1.080	60.0		112.2	116.0
V	1.514	1.354	1.080	60.0		112.2	116.0
VI	1.514	1.354	1.080	60.0		112.2	116.0

resulting from substitution. This technique would be successful and efficient for all the molecules discussed in this article but, for the reasons cited at the beginning of this paragraph, we have only employed it when the other schemes fail. Charge density difference plots have been used by researchers for many years. For example, Bader et al.[20] calculated density difference maps for several diatomic molecules to investigate charge redistributions upon molecular formation. More recently, Morokuma[21] has calculated charge density difference plots for the various terms in his hydrogen bond energy decomposition scheme. Payne and Allen[22] have used density difference maps to probe the rotational barrier mechanisms in ethane, propane, and methylamine.

Another result of this work (the proof of which is given in section IIID) is a simple additivity rule which is easy to apply and helps systemize conclusions from the charge density difference plots. For example, the pattern of bond length changes in 1,1-difluorocyclopropane may be added to a copy of the same pattern rotated by 60° to predict bond length changes in 1,1,2,2-tetrafluorocyclopropane. A second example is rationalization of the observed bond length changes for *cis*-1,2,3-trifluorocyclopropane.[16]

In a previous paper,[1] we reported semiempirical calculations for cyclopropane and cyclopropanone which resulted in a reasonable match to the ab initio calculations. We have carried out INDO calculations for 1,1-difluorocyclopropane and obtained the same conclusion. These computations are easily made on most digital computers and to save space detailed results are not tabulated. For those interested, these numbers may be obtained directly from the authors.

II. Computational Details

Ab initio LCAO-MO-SCF wave functions were determined for all six molecules utilizing the GAUSSIAN 70 computer program and the minimal STO-3G s, p basis set[27,28] on an IBM 360-91 computer. Molecules I and II were also calculated with the INDO semiempirical scheme.[29]

Although the STO-3G basis set is fairly inaccurate in reproducing the geometries,[30] force constants,[30] and electric dipole moments[27] of fluorocarbons, trends in these molecular properties for a series of related fluorocarbons are reproduced satisfactorily. Even though electric dipole moments are too small[27] and F → C back-bonding and charge alternation[27,31] are exaggerated, the relative charge distributions yield a reasonable representation.

Rohmer and Roos[6] and Hariharan and Pople[32] have investigated the role of d functions in strained cyclic systems. They conclude that d functions are required for a complete and accurate description of the electronic structure in three-membered rings. But Rohmer and Roos[6] find that polarization functions do not contribute to substituent effects. It follows then that the STO-3G s, p basis set is adequate for our purposes.

Geometry Choice. Molecules II-VI were calculated at the experimental C-C and C-H bond lengths and the C-C-C and C-C-H bond angles of I.[12] C-F bond distances and F-C-F bond angles in II and III are the experimental values for II.[15] C-F bond lengths and H-C-F bond angles in IV-VI are the values determined experimentally for VI[16] (Table I gives all geometries). This choice of geometries was based on an approach used by Hoffmann et al.[5] who pointed out that comparison of Mulliken overlap populations[32] should then reflect whether the substituents weaken or strengthen the ring bonds.

Charge Density Difference Plots. A cogent point concerning overlap populations has been made by Bader et al.[20] They note that an interpretation of bonding based solely on population analysis can be misleading, since bonding depends not only on the amount of charge in the bond, but also on its disposition, i.e., whether it is diffuse or concentrated. The same value of the overlap population might be obtained with one set of orbitals pointed along an internuclear axis and a second set pointing at an angle to the axis, but the actual strength of the bond would be different in the two cases. Therefore, in order to test and supplement overlap population comparisons we have obtained charge density difference plots.

Two sets of charge density differences maps were generated from the ab initio wave functions using a program written at Princeton by W. L. Jorgensen. The first set compares 1,1-difluorocyclopropane (II) with cyclopropane (I); the second compares 1,1,2,2-tetrafluorocyclopropane (III) with cyclopropane (I). These charge density difference plots are particularly useful, since the cyclopropane ring geometry has been retained in the substituted molecules; thus the maps reflect only the charge redistributions and accompanying forces acting on the ring nuclei which result from substitution. Each of the six plots represents charge density differences in the $Y = 0.0$ plane, i.e., the plane containing the ring nuclei. The plots were computed by subtracting the valence MO's of I from the corresponding valence orbitals of II and III for SS symmetry,[25] SA symmetry,[25] and the sum of all MOs. Contour maps were also obtained for molecular cross sections in the $Y = 1.5$ and $Y = 1.9$ au planes to determine whether the substituent-parent molecule interaction produces significant charge redistributions outside of the molecular plane. These maps show that charge redistributions in planes other than the molecular plane contribute little to the substituent effects; therefore, we have omitted them from this paper. This result was not unexpected, since Bader et al.[20] have pointed out that only charge transfers along bond axes generate effective forces on the nuclei.

A logarithmic contour scale was used in the plots. The contour values are listed in Table II. We have followed the standard convention: solid lines delineate regions of increase, dashed lines regions of decrease.

III. Results and Analysis of Results

A. Charge Distributions. Atomic charges from population analysis[33] are given below for molecules I-VI. The following

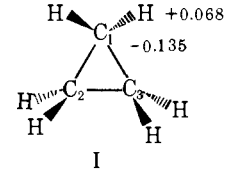

I

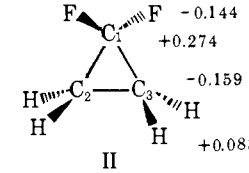

II

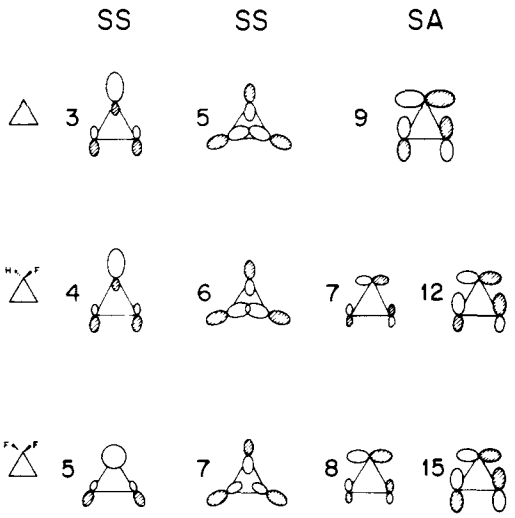

Figure 1. Molecular orbital diagrams for fluoro substitution of cyclopropane. The orbitals are classified according to the reflections in the plane of the molecule and perpendicular to it (SS, SS, SA).[25] Related orbitals of a given type are shown vertically under the symmetry heading.

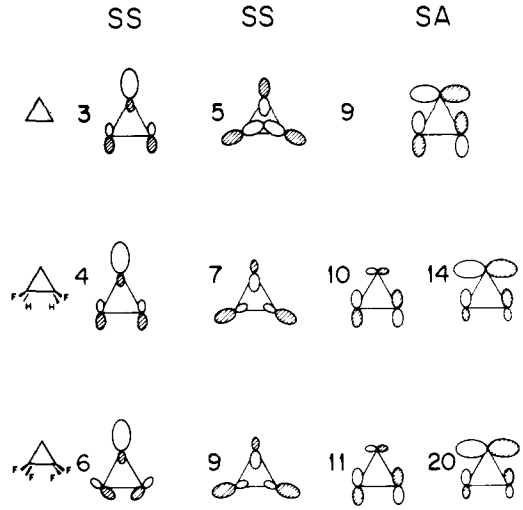

Figure 2. Molecular orbital diagrams for fluoro substitution of cyclopropane. The orbitals are classified according to the reflections in the plane of the molecule and perpendicular to it (SS, SS, SA).[25] Related orbitals of a given type are shown vertically under the symmetry heading.

Table II, Values of Contours for Difference Plots (e/au^3)

No.	Density	No.	Density	No.	Density
−9	−1.000 00	−2	−0.000 32	4	0.003 16
−8	−0.316 20	−1	−0.000 10	5	0.010 00
−7	−0.100 00	0	0.000 00	6	0.031 62
−6	−0.031 62	1	0.000 10	7	0.100 00
−5	−0.010 00	2	0.000 32	8	0.316 20
−4	−0.003 16	3	0.001 00	9	1.000 00
−3	−0.001 00				

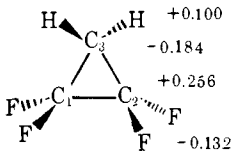

III

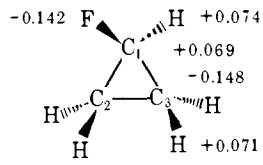

IV

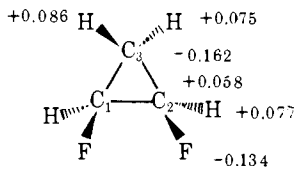

V

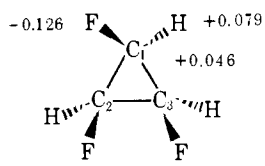

VI

observations can be made upon examining these diagrams. (1) Replacing one or both hydrogens on a carbon produces the same pattern of charge changes, but the magnitudes of the changes differ. For molecules II and IV, C(1) and the H's are more positive and C(2) and C(3) are more negative than these atoms are in I. Both substitutions are causing an alternating charge distribution,[27,31] but the charge changes on II are twice those on IV. For molecules III and V, C(1) and C(2) are both more positive than these carbons are in I. Similarly, the charge transfers in V which bring about the alternating charge distribution are in the same direction as those in III, but smaller by one half. (2) Comparing the charges on the carbons in II with those in I yields the following charge gains and losses due to difluoro substitution (a minus sign indicates charge loss and a plus sign gain). If one assumes that the charge changes in III result from a superposition of the charge changes in II, the

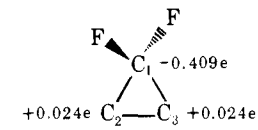

following gains and losses are predicted (eq 1), while the actual

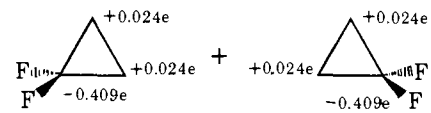

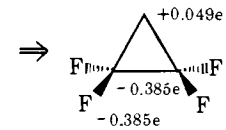

(1)

values are shown below. It is immediately apparent that ad-

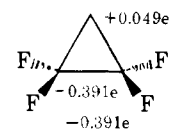

ditivity is a successful postulate. The same conclusion is obtained for IV and V.

B. Orbital Compositions, Orbital Energy Correlation Diagrams, and Overlap Populations. The MO's predominantly affected by the substituents are shown schematically in Figures 1 and 2. For the substituted molecules these are the symmetry allowed bonding and antibonding combinations of the substituent orbitals mixed with the parent molecules. For II and IV, SS[25] and S symmetry leads to one relevant combination; SA and A produces two. For III and V, SS and S and SA and A both lead to two relevant combinations.

Figure 3 is an orbital energy correlation diagram for molecules I, II, and IV. This diagram also shows which parent molecule orbitals are affected by substitution and their relative stabilities. The corresponding diagram for molecules I, III, and V has not been included, since it is too complicated for easy analysis.

Figures 1 and 2 show that compared to I molecules II and IV (and III and V) have the same pattern of atomic orbital (AO) coefficient changes for MOs 3, 5, and 9. Figure 3 dem-

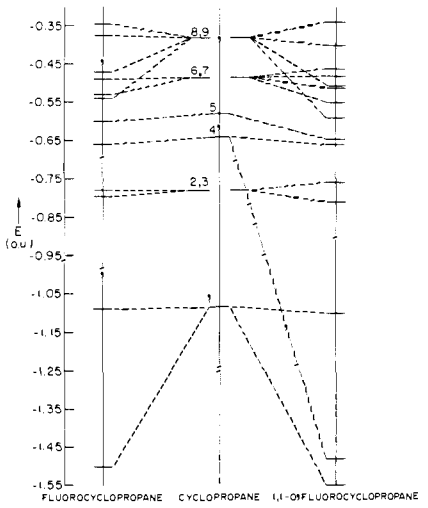

Figure 3. Orbital energy correlation diagrams for monofluoro (left) and difluoro (right) addition to cyclopropane.

onstrates the basic commonality in the energy level splitting diagrams for molecules II and IV. The overlap populations (Tables III-V) show that analogous mono- and disubstituted cyclopropanes have parallel overlap changes compared to I. Together with the trends in the charge redistributions described previously, the above statements demonstrate that replacing one or two hydrogens on a carbon leads to modifications in cyclopropane molecular properties in the same direction, but the changes induced by one fluorine are smaller than those induced by two. This implies that any conclusions drawn about the origin and consequences of the substituent effects in II (III) are also applicable to IV (V). However, the fluorine induced geometry changes in the cyclopropane ring will be greater for II (III) than for IV (V).

Cyclopropane, Fluorocyclopropane, and 1,1-Difluorocyclopropane. The C(2)–C(3) Bonds. By examining the coefficient changes produced in each cyclopropane MO upon substitution, it is apparent that MO 9 (SA symmetry) is the orbital of cyclopropane principally involved in induced C(2)-C(3) bond length change. As shown in Figure 1 fluorine-MO 9 interactions increase the charge density on C(2) and C(3) in MO 9, leading to an increase in the antibonding interaction between these carbons and thus to C(2)-C(3) bond weakening. The overlap populations of Table IV also show that cyclopropane orbitals of SA symmetry are responsible for the C(2)-C(3) weakening. Total overlap populations (Table V) likewise indicate that substitution produces a decrease in the overlap population (bond weakening) of the C(2)-C(3) bond in cyclopropane. The orbital energy splitting diagram (Figure 3) shows that these interactions are stabilizing. Therefore, the C(2)-C(3) bonds in molecules II and IV should be longer than the C-C bonds in I with the C(2)-C(3) bond lengthening in II greater than that IV. This conclusion agrees with the experimental results for I and II.[12,15]

The C(1)–C(2,3) Bonds. The orbitals of cyclopropane primarily involved in the fluorine induced changes in the C(1)-C(2,3) bonds are MOs 1, 3, and 5. Figure 1 shows that fluorine interaction with MO 3 of cyclopropane will strengthen the C(1)-C(2,3) bonds, while interaction with MO 5 of cyclopropane will weaken these bonds. The interaction with MO 3 strengthens the adjacent bonds by reducing the antibonding overlap in this cyclopropane orbital and by directing the charge density more nearly along the bond axis.[20]

The interaction of the fluorine with MO 1 of cyclopropane also strengthens the adjacent bonds by increasing the C(1)-C(2,3) bonding overlap. (We have not included MO 1 in Figure 1, since the adjacent bond strengthening produced via MOs 1 and 3 is in the same direction and is brought out more clearly by MO 3.)

The fluorines induce adjacent bond weakening via MO 5 of cyclopropane by decreasing the magnitude of the charge density in the bonding region, thereby reducing the bond overlap.

The orbital energy splitting diagram (Figure 3) enables us to determine whether the fluorine-MO 1, MO 3 or fluorine-MO 5 interactions will dominate.[34] Figure 3 shows that the F-MO 1 and F-MO 5 interactions are stabilizing, while the F-MO 3 interaction is destabilizing for both molecules II and IV. The orbital energy changes resulting from the F-MO 3 and F-MO 5 interactions nearly cancel each other, leaving the orbital energy change resulting from the F-MO 1 interaction as the dominant influence. Thus the adjacent bonds will shorten in both II and IV, but the C(1)-C(2,3) bonds in IV will not shorten as much as they do in II. This conclusion agrees with the experimental results.[12,15]

In contrast to the results for the C(2)-C(3) bonds, the Mulliken overlap populations are an invalid measure for the C(1)-C(2,3) bonds. Table V implies that the C(1)-C(2,3) bonds in the substituted molecules II and IV should be longer than the C-C bonds in I. The reason for the overlap population

Table III. C(1)-C(2,3)[a] or C(3)-C(1,2)[b] Bond Overlap Populations for Valence Orbitals

Molecule	SS[c] (S)[d]	SA[c] (A)[d]	AS[c] (S)[d]	AA[c] (A)[d]
I	0.308	0.294	−0.003	0.000
II	0.280	0.284	0.004	0.000
III	0.243	0.285	0.005	0.000
IV	0.282	0.287	0.017	0.003
V	0.291	0.251	−0.008	0.038
VI	0.275	0.292	0.017	0.005

[a] For molecules I, II, IV, and VI. [b] For molecules III and V. [c] For molecules I, II, and III.[25] [d] For molecules IV, V, and VI.[25]

Table IV. C(2)-C(3)[a] or C(1)-C(2)[b] Bond Overlap Populations for Valence Orbitals

Molecule	SS[c] (S)[d]	SA[c] (A)[d]	AS[c] (S)[d]	AA[c] (A)[d]
I	0.855	−0.253	0.100	−0.113
II	0.851	−0.282	0.113	−0.116
III	0.792	−0.273	0.095	−0.090
IV	0.856	−0.268	0.111	−0.112
V	0.836	−0.269	0.138	−0.141
VI	0.854	−0.287	0.109	−0.126

[a] For molecules I, II, IV, and VI. [b] For molecules III and V. [c] For molecules I, II, and III.[25] [d] For molecules IV, V, and VI.[25]

Table V. Total Bond Overlap Populations[a]

Molecule	C(1)-C(2,3)[b] (C(3)-C(1,2))[c]	C(2)-C(3)[b] (C(1)-C(2))[c]	C-F
I	0.596	0.596	
II	0.565	0.563	0.434
III	0.531	0.519	0.430
IV	0.580	0.584	0.444
V	0.570	0.560	0.442
VI	0.549	0.549	0.440

[a] The total overlap populations may not be exactly equal to SS + SA + AS + AA in Tables II and IV, since those values represent only the valence orbitals. [b] For molecules I, II, IV, and VI.[25] [c] For molecules III and V.[25]

failure is the greater overlap loss on substitution in MO 5 compared to the overlap gain in MO 1 and MO 3. For MO 5 (Figures 1 and 2) substitution of cyclopropane creates overlap changes in the center of the ring; for MO 3 they are along the C-C bond axes. The potential energy is higher in the ring center than along the internuclear axis; thus a given change in overlap in the ring center represents a significantly lower bond strength change than the same change along the internuclear line. This follows the observation of Bader et al.[20] that bonding interpretations based on overlap population can be misleading because this analysis considers only the amount of charge density in the bonding region and not its special placement.

Examination of orbital composition schematics enables one to anticipate when an overlap population criteria of bond strength is likely to fail. It is clear that this will happen in strained rings and the following are examples: (1) Rohmer and Roos[6] in the series of molecules A-C;

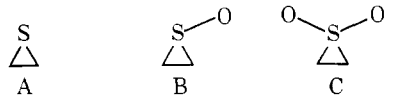

(2) Lehn and Wipff[35] on bicyclo[2.1.1]hexane and bicyclo[1.1.1]pentane; (3) Newton and Schulman[36] on bicyclobutane.

Cyclopropane, *cis*-1,2-Difluorocyclopropane, and 1,1,2,2-Tetrafluorocyclopropane. The orbital diagrams given in Figure 2 suggest the SS (S) and SA (A) symmetry orbitals as the pertinent MOs involved in the substituent induced geometry changes. However, we can not proceed further in the analysis with either Mulliken overlap populations or orbital energy correlation diagrams. Overlap populations are invalid for the reasons given above. The correlation diagrams fail because their complexity makes it too difficult to locate the controlling orbitals. Thus, another technique is required to quantify the suggestion based on orbital composition. The charge density difference plots discussed below provide the necessary information in a usable and convenient form.

C. Charge Density Difference Plots. The charge density difference plots comparing 1,1-difluorocyclopropane (II) with cyclopropane (I) are given in Figure 4. The plots comparing 1,1,2,2-tetrafluorocyclopropane (III) with cyclopropane (I) are given in Figure 5.

In order to illustrate how charge density difference plots can aid our analysis, we return to the difficulties found in overlap populations and orbital energy correlation diagrams discussed in the two paragraphs above. Figures 4A and 4B are the difference maps of 1,1-difluorocyclopropane minus cyclopropane for the sum of SS and SA valence orbitals, respectively. SA orbitals govern C(2)-C(3) bond length and we note that Figure 4B has a simple pattern and all regions show a charge gain. There is little charge buildup between C(2) and C(3), but considerable behind them (just the charge distribution we expect from enhanced C(2)-C(3) antibonding in dominant orbital, MO 9). Because of the inherent simplicity of the charge density difference plot, it is not surprising that overlap populations lead to a correct prediction in this case. In contrast, the several changes from loss to gain in Figure 4A and its rather complex composite of bulging contours, which do not follow the internuclear axes, make it clear why the uncritical spacial averaging intrinsic to overlap population can lead to an invalid measure. It is also easy to appreciate that for large systems charge density difference maps are at an advantage compared to the overly intricate orbital energy correlation diagrams, since the maps employ a sum over many orbitals.

The interpretation of charge density difference maps is carried out by dividing up the plot into regions around the atoms and assigning a resultant force to each nuclei. In selecting regions the investigator automatically adds information to the analysis from his chemical experience.

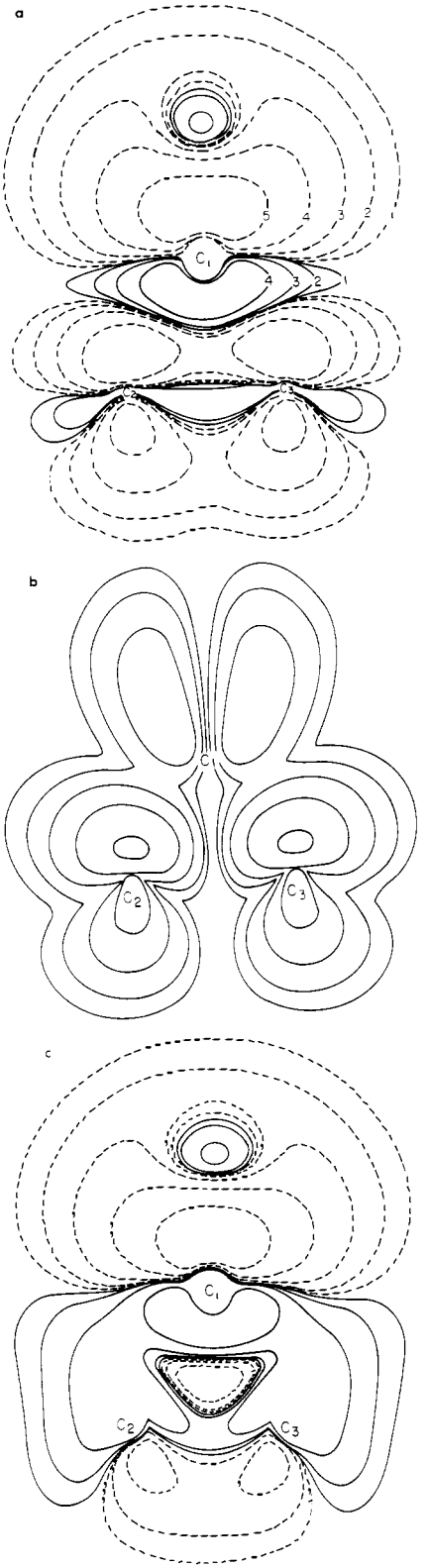

Figure 4. Charge density difference plots (a) subtracting the SS symmetry valence orbitals of cyclopropane from the SS symmetry valence orbitals of 1,1-difluorocyclopropane; (b) subtracting the SA symmetry valence orbitals of cyclopropane from the SA symmetry valence orbitals of 1,1-difluorocyclopropane; and (c) subtracting the sum of all the cyclopropane valence MO's from the sum of all the 1,1-difluorocyclopropane valence MO's. The plot represents charge density differences in the $Y = 0.0$ plane, i.e., the plane containing the ring nuclei. A logarithmic contour scale was used. Solid lines delineate regions of increase; dashed lines delineate regions of decrease.

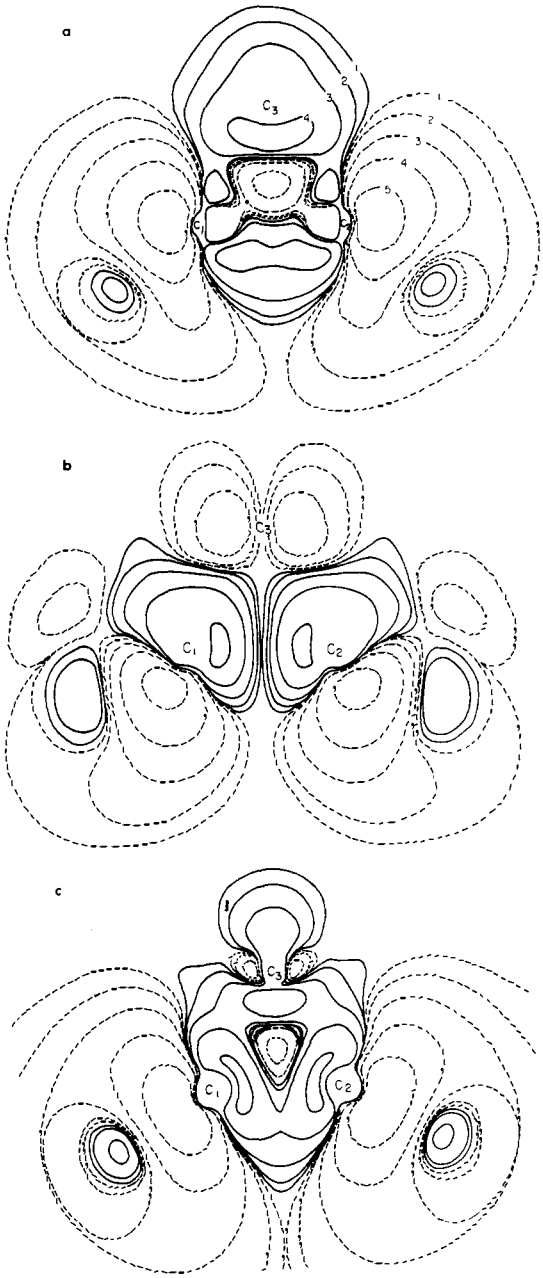

Figure 5. Charge density difference plots: (a) subtracting the SS symmetry valence orbitals of cyclopropane from the SS symmetry valence orbitals of 1,1,2,2-tetrafluorocyclopropane; (b) subtracting the SA symmetry valence orbitals of cyclopropane from the SA symmetry valence orbitals of 1,1,2,2-tetrafluorocyclopropane; and (c) subtracting the sum of all the cyclopropane valence MO's from the sum of all the 1,1,2,2-tetrafluorocyclopropane valence MO's. The plot represents charge density differences in the $Y = 0.0$ plane, i.e., the plane containing the ring nuclei. A logarithmic contour scale was used. Solid lines delineate regions of increase; dashed lines delineate regions of decrease.

Since the Hellmann-Feynman theorem[37] relates the electronic charge distribution to the forces acting on the nuclei, it is instructive to analyze the effect of the substituent induced charge redistributions in terms of the forces exerted on the ring carbons. The concepts involved are:[20] (1) Charge increase in the region between the nuclei increases screening of the nuclear charges and creates an attractive force which draws the nuclei together. (2) Charge loss between the nuclei and built up on the backside of the nuclei deshields the nuclear charges and pulls the nuclei apart. (3) Charge transferred into the region along the internuclear axis is most effective in shortening the bond. (4) A diffuse charge transfer above and below the bond into an s or π orbital is relatively ineffective in shortening the bond. Deb[38] and Nakatsuji[39] have also used analysis based on the Hellmann-Feynman theorem to predict molecular geometries.

Fluorine substitution of cyclopropane generates charge redistributions and forces which shift the substituted carbon toward the opposite bond and draws the unsubstituted carbons apart and up toward the substituted one. The charge density difference plots reveal the group of symmetry orbitals[25] responsible for the pertinent charge redistributions; the orbital compositions and overlap populations bring out the dominant MO within the relevant group.

Fluorocyclopropane and 1,1-Difluorocyclopropane. The total charge density redistribution in cyclopropane induced by difluoro substitution is presented in Figure 4C and schematically below. The region around C(1) shows a charge loss between

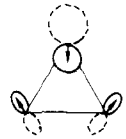

4C

C(1) and the F's which forces them apart and moves C(1) toward the C(2)-C(3) bond. Charge is built up behind C(2) and C(3) and in the C(1)-C(2,3) bonds, drawing C(2) and C(3) apart and up toward C(1). Figure 4A and the schematic below demonstrate that the force acting on C(1) arises primarily from the charge redistributions in the SS symmetry orbitals.[25] The charge loss above and below C(2) and C(3) and the gain behind them offsets the gain along the C(2)-C(3) bond so that C(2) and C(3) do not move. The charge shifts

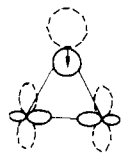

4A

which displace C(2) and C(3) originate from SA symmetry orbitals[23] (Figure 4B and schematic below). The compromise

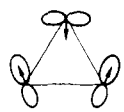

4B

between the charge buildup in the C(1)-C(2,3) bonds and C(1)-F bonds pulls C(1) slightly toward the C(2)-C(3) bond. The small charge gain between C(2) and C(3) and the significant buildup behind C(2) and C(3) pulls these atoms apart. The net effect of these carbon rearrangements is shorter C(1)-C(2,3) (adjacent) bonds and a longer C(2)-C(3) (opposite) bond in II than in I. This conclusion is completely consistent with the experimental results for I[12] and II,[15] demonstrating that charge density difference plots are a useful predictive tool for this research. It also confirms the analysis in sections A and B that the interaction between the fluorines and MO 1 and MO 3 (SS symmetry) of cyclopropane is primarily responsible for the movement of C(1) (Figures 4A and 4C).

The fluorine-MO 1 interaction transfers charge from the C(1) 2s AO to the C(1) 2pz AO; the fluorine-MO 3 interaction transfers charge from C(1) to C(2) and C(3). Both charge transfers displace C(1) downward. Thus, the charge alternation effect[27,31] induced in the σ orbitals by the fluorine appears to be a factor in adjacent bond shortening.

The analogous interaction with MO 9 (SA symmetry) of cyclopropane accounts for the C(2,3) displacements derived

from Figures 4B and 4C. As noted in section B, this interaction leads to an increase in the antibonding charge density between C(2) and C(3) and pushes them apart. Hoffmann et al.[5] have cited the same substituent-parent molecule MO interaction as the source of opposite bond lengthening in the series of molecules, A-C.

As noted above, the changes in charge distributions (part A), orbital diagrams (Figure 1), and overlap populations (Tables III-IV) for II and IV (compared to I) indicate that the bond length changes for IV are approximately half as large as those for II, yielding the following geometry.

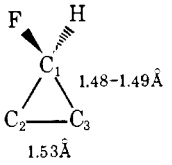

IV

Having established the reliability of charge density difference plots in manifesting bond length changes, we now turn to the contour maps in Figure 5, where the geometry of one of the compounds (III) has not been entirely determined experimentally.[26]

***cis*-1,2-Difluorocyclopropane and 1,1,2,2-Tetrafluorocyclopropane.** The total charge density redistribution in cyclopropane induced by tetrafluoro substitution is given in Figure 5C and schematically below. There is a charge loss between

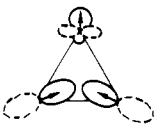

5C

C(1) and F and between C(2) and F which pushes the carbons toward the opposite ring bond, and there is a charge gain between C(1) and C(2) which pulls them together. Overall, C(1) and C(2) are displaced inward above the internuclear axis. The force acting on C(3) is less obvious due to the charge buildup in front of and behind this carbon. However, this pattern of charge redistribution is very similar to the pattern found for Be in Be_2 upon "molecular formation".[20] This suggests that the charge gain on the backside of C(3) and the polarization of the atomic charge distribution in the same direction will dominate the charge gain in front of C(3), drawing C(3) away from the C(1)-C(2) bond.

Figure 5A and the schematic shown below demonstrate that the overall charge buildup in front of and behind C(3) arises from the charge rearrangements in the SS symmetry orbitals.

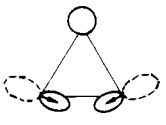

5A

The charge loss on either side of this carbon observed in Figure 5C is due to the charge shifts in the SA symmetry orbitals (Figure 5B and schematic below). With respect to C(1) and

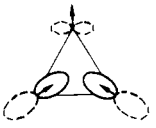

5B

C(2), the charge redistributions in the SA symmetry orbitals create forces which draw C(1) and C(2) together above the internuclear axis. In Figure 5C these forces have been modified somewhat by the forces arising from the SS symmetry orbitals, which pull these carbons together below the bond axis. The net effect of these carbon rearrangements is a shortening of the C(1)-C(2) bond and essentially no change in the C(3)-C(1,2) bonds. This theoretical result for the C(1)-C(2) bond agrees with the experimental result obtained by Stigliani and Laurie.[26]

As for II and IV, the changes in charge distributions (part A), orbital diagrams (Figure 2), and overlap populations (Tables III-V) for III and V (compared to I) suggest that the C(1)-C(2) bond length in V should be midway between those in I and III.

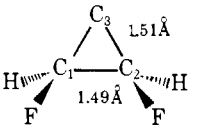

V

The orbital diagrams (Figure 2) indicate that the interaction between the fluorines and MO 3 (SS symmetry) and MO 9 (SA symmetry) of cyclopropane are primarily responsible for the rearrangement of the carbons in III and V. The C(1)-C(2) bond shortening arises from (1) the modification of the charge density distribution between C(1) and C(2) in MO 3, which directs it more along the internuclear axis; and (2) the decrease in the antibonding charge density between C(1) and C(2) in MO 9. The C(3)-C(1,2) bond lengths are essentially unchanged due to two opposite effects: (1) the decrease in the antibonding character of these bonds in MO 3; and (2) the decrease in the bonding character of these bonds in MO 9.

D. Additivity Rule. The atomic charge distributions for molecules I-VI (Results section) suggest that successive fluorination of cyclopropane modifies its molecular properties in an additive manner. If this hypothesis is correct, the forces acting on the carbons in molecule III can be derived from the following vector sum (Scheme I below) of the forces acting on

Scheme I

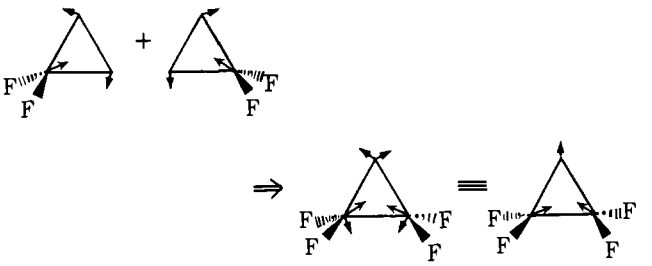

the carbons in molecule II (schematic 4C). Comparing the last diagram in Scheme I with schematic 5C shows that they are identical, verifying the additivity postulate.

Scheme I is based on molecules II and III, but is also applicable to IV-VI, since we have shown that a single fluorine substitution creates forces in the same directions (but of smaller magnitude) as those present in the difluoro case. Scheme II utilizes the additivity principle to deduce the the-

Scheme II

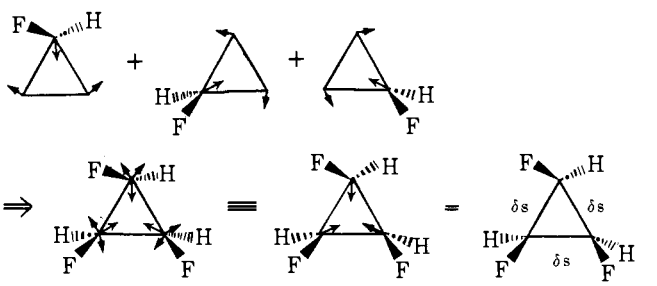

oretical bond length changes in VI. The result is completely consistent with the experimentally observed C-C bond distance of 1.507 Å[16] (a bond length change of 0.01 Å). We conclude,

therefore, that once it is known how one fluorination affects the molecular properties of cyclopropane (I), the effect of two, three, . . . , fluorinations is readily determined.

The additivity principle (Schemes I and II) can be represented as a simple *scalar* superposition rule for molecules II-VI and this makes the results easy to remember and apply (Scheme III). Here s = shorten, l = lengthen, and u = unchanged, and the symbols represent changes in these bond lengths with respect to the bond lengths in cyclopropane (I).

Scheme III

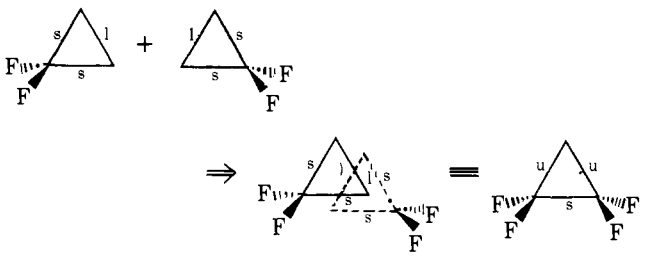

E. Generalization to Other Systems. Since the above analysis of cyclopropane substituent effects is based solely on induced charge transfer, it should be general for electronegative substituents. This is verified by the observation that our approach explains the bond length changes in the cyclopropane ring due to F, O,[1] and CH_2[1] substitution. The differential bond shortening and lengthening in these substituted molecules results from the variations in the strength of the substituent-cyclopropane MO 9 interaction. This interaction tends to lengthen the opposite bond (C(2)-C(3)) substantially and the adjacent bonds (C(1)-C(2,3)) slightly. Therefore, the larger this mixing is the more the C(2)-C(3) bond lengthens and the less the C(1)-C(2,3) bonds shorten. Since the relative magnitude of the substituent-MO 9 interaction is O > F > CH_2,[1] the relative shortening of the adjacent bond follows the order CH_2 > F > O, whereas the relative lengthening of the opposite bond follows the order O > F > CH_2.

Since chlorine is an electronegative atom, our analysis is also applicable to chlorine-substituted cyclopropane (ignoring steric effects). There are two conflicting sets of bond lengths for 1,1-dichlorocyclopropane in the literature.[17,18] The earlier experimental values[17] indicate that all three cyclopropane ring bonds lengthen upon dichlorination. The more recent data[18] indicate that the C(2)-C(3) bond lengthens, but the C(1)-C(2,3) bonds shorten. Our theoretical analysis yields bond length changes which agree with those obtained in the later work, suggesting that those results are more accurate.

Our approach also enables us to explain the observed bond length differences in 1,1-difluorocyclopropene[23] and cyclopropene.[24] Cyclopropene has one less orbital than cyclopropane. Jorgensen and Salem[8] have shown that the AA symmetry orbital (MO 6) of cyclopropane is the orbital which has no counterpart in cyclopropene. We demonstrated above that only the charge redistributions in the cyclopropane SS and SA symmetry orbitals make a significant contribution to the cyclopropane substituent effects. Therefore, all of the pertinent cyclopropane orbitals are represented in cyclopropene, and our analysis is relevant. The bond length changes for 1,1-difluorocyclopropene obtained from our theoretical approach will parallel those obtained for 1,1-difluorocyclopropane. This result agrees with the changes found experimentally.[12,15,23,24]

IV. Summary

In summary, we have made the following points: (1) Fluorine substitution of cyclopropane generates charge redistributions which move the substituted carbon toward the opposite bond and draw the unsubstituted carbons apart and up toward the substituted carbon. (2) The charge density difference plots point to the group of symmetry orbitals responsible for the pertinent charge redistributions; the orbital compositions and overlap populations point to the dominant MO within the relevant group. (3) Successive fluorination of cyclopropane modifies its molecular properties in an additive manner which follows a simple scalar superposition rule. (4) Our analysis of cyclopropane substituent effects is general for electronegative groups. It is also applicable to cyclopropene. (5) The same general conclusions arise from the STO-3G and INDO calculations.

Note Added in Proof. N. J. Fitzpatrick and M. O. Fanning have carried out ab initio (STO-3G) geometry optimized calculations on a series of disubstituted cyclopropanones, *J. Mol. Struct.*, **25,** 197 (1975); **33,** 257 (1976). The pattern of geometries and charge distributions they find are in agreement with those to be expected from the analysis given here. It is interesting to note that they also obtain Mulliken overlap populations which are not simply correlated with bond lengths.

Acknowledgment. The authors would like to thank the Biophysics Program, Biochemistry and Physiology Section of the National Science Foundation for support through Grant BMS73-06999.

References and Notes

(1) C. A. Deakyne, V. W. Laurie, and L. C. Allen, *J. Am. Chem. Soc.*, **99**, 1343 (1977).
(2) R. Hoffmann, *J. Am. Chem. Soc.*, **90**, 1475 (1968).
(3) R. Hoffmann, *Tetrahedron Lett.*, 2097 (1970).
(4) R. Hoffmann and W.-D. Stohrer, *J. Am. Chem. Soc.*, **93**, 6941 (1971).
(5) R. Hoffmann, H. Fujimoto, J. R. Swenson, and C.-C. Wan, *J. Am. Chem. Soc.*, **95**, 7644 (1973).
(6) M.-M. Rohmer and B. Roos, *J. Am. Chem. Soc.*, **97**, 2025 (1975).
(7) R. C. Haddon, *Tetrahedron Lett.*, 2797 (1974).
(8) W. L. Jorgensen and L. Salem, "The Organic Chemist's Book of Orbitals", Academic Press, New York, N.Y., 1973.
(9) J. G. Burr and M. J. S. Dewar, *J. Chem. Soc.*, 1201 (1954).
(10) N. Bodor, M. J. S. Dewar, A. Harget, and E. Haselbach, *J. Am. Chem. Soc.*, **92**, 3854 (1970).
(11) J. F. Olsen, S. Kang, and L. Burnelle, *J. Mol. Struct.*, **9**, 305 (1971); J. F. Olsen and S. Kang, *ibid.*, **9**, 315 (1971).
(12) W. J. Jones and B. P. Stoicheff, *Can. J. Phys.*, **42**, 2259 (1964).
(13) J. M. Pochan, J. E. Baldwin, and W. H. Flygare, *J. Am. Chem. Soc.*, **91**, 1896 (1969).
(14) V. W. Laurie and W. M. Stigliani, *J. Am. Chem. Soc.*, **92**, 1485 (1970).
(15) A. T. Perretta and V. W. Laurie, *J. Chem. Phys.*, **62**, 2469 (1975).
(16) C. W. Gillies, Spectroscopy Meetings in Columbus, Ohio, 1975, on microfilm.
(17) W. H. Flygare, A. Narath, and W. D. Gwinn, *J. Chem. Phys.*, **36**, 200 (1962).
(18) K. C. Cole and F. R. Gilson, *J. Mol. Struct.*, **28**, 385 (1975).
(19) R. H. Schwendemann, G. D. Jacobs, and T. M. Krigas, *J. Chem. Phys.*, 40, 1022 (1964).
(20) R. F. W. Bader, W. H. Henneker, and P. E. Cade, *J. Chem. Phys.* **46**, 3341 (1967); R. F. W. Bader, I. Keaveny, and P. E. Cade, *J. Chem. Phys.*, 47, 3381 (1967).
(21) S. Yamabe and K. Morokuma, *J. Am. Chem. Soc.*, **97**, 4458 (1975).
(22) P. W. Payne and L. C. Allen, "Charge Density Difference Analysis. 1. Comparison of Bonding and Rotational Barriers in Ethane and Propane", submitted to *J. Am. Chem. Soc.*; P. W. Payne and L. C. Allen, "Charge Density Difference Analysis. 2. Comparison of Rotational Barriers in Ethane and Methylamine", submitted to *J. Am. Chem. Soc.*
(23) K. R. Ramaprasad, V. W. Laurie, and N. C. Craig, *J. Chem. Phys.*, **64**, 4832 (1976).
(24) W. M. Stigliani, V. W. Laurie, and J. C. Li, *J. Chem. Phys.*, **62**, 1890 (1975).
(25) The molecular orbitals for molecules II and III have been classified with respect to two symmetry planes. The first symbol represents the symmetry of the MO with respect to the plane of the molecule, i.e., whether it is symmetric (S) or antisymmetric (A). The second symbol represents the orbital symmetry with respect to the plane perpendicular to the molecular plane passing through C(1) and bisecting the C(2)–C(3) bond in II. The overall symmetry of these molecules leads to four different sets of orbital symmetries, SS, SA, AS, and AA. The overall symmetry of molecules IV–VI is lower than that of molecules II and III. The only plane of symmetry for IV–VI is the plane perpendicular to the plane of the ring passing through C(1) and bisecting the C(2)–C(3) bond in IV. Thus, the molecular orbitals in these compounds are classified as simply symmetric (S) or antisymmetric (A) with respect to this plane. However, despite the lower symmetry of molecules IV–VI, it is still possible to correlate the MOs of these molecules with those of molecules I, II, and III, since the composition of the MOs has only changed slightly.
(26) W. M. Stigliani and V. W. Laurie, private communication. These authors

have carried out a microwave study of 1,1,2,2-tetrafluorocyclopropane, which yields a value of 1.47 Å for the C(1)–C(2) bond distance. The C(3)–C(1,2) bond lengths could not be determined due to the unfavorable position of the center of mass.
(27) W. J. Hehre and J. A. Pople, *J. Am. Chem. Soc.*, **92**, 2191 (1970).
(28) W. J. Hehre, R. F. Stewart, and J. A. Pople, *J. Chem. Phys.*, **51**, 2657 (1969); W. J. Hehre, R. Ditchfield, R. F. Stewart, and J. A. Pople, *ibid.*, **52**, 2769 (1970).
(29) J. A. Pople and G. A. Segal, *J. Chem. Phys.*, **44**, 3289 (1966); D. P. Santry and G. A. Segal, *ibid.*, **47**, 158 (1967).
(30) M. D. Newton, W. A. Lathan, W. J. Hehre, and J. A. Pople, *J. Chem. Phys.*, **52**, 4064 (1970).
(31) J. A. Pople and M. S. Gordon, *J. Am. Chem. Soc.*, **89**, 4253 (1967); L. Radom, W. J. Hehre, and J. A. Pople, *ibid.*, **94**, 2371 (1972).
(32) P. C. Hariharan and J. A. Pople, *Chem. Phys. Lett.*, **16**, 217 (1972).
(33) R. S. Mulliken, *J. Chem. Phys.*, **23**, 1833, 1841, 2338, 2343 (1955).
(34) A. D. Walsh, *J. Chem. Soc.*, 2260, 2266, 2288, 2296, 2301 (1953); A. D. Walsh, *Prog. Stereochem.*, **1**, 1 (1954).
(35) J. M. Lehn and G. Wipff, *Theor. Chim. Acta*, **28**, 223 (1973); *Chem. Phys. Lett.*, **15**, 450 (1972).
(36) M. D. Newton and J. M. Schulman, *J. Am. Chem. Soc.*, **94**, 767 (1972).
(37) R. P. Feynman, *Phys. Rev.*, **56**, 340 (1939); H. Hellmann, "Einfuhrung in die Quantenchemie", Franz Deutlcke, Leipzlg, E. Germany, 1937, pp 285ff.
(38) B. M. Deb, *J. Am. Chem. Soc.*, **96**, 2030 (1974).
(39) H. Nakatsuji, *J. Am. Chem. Soc.*, **95**, 345, 354 (1973).

On the Theory of Phase-Transfer Catalysis[1]

John E. Gordon* and Raymond E. Kutina

Contribution from the Department of Chemistry, Kent State University, Kent, Ohio 44242. *September 10, 1976*

Abstract: Two-phase reactions run under phase-transfer catalysis (PTC), such as RX(org) + Y^-(aq) → RY(org) + X^-(aq), are treated as sums of the rate-limiting, homogeneous reactions RX(org) + Y^-(org) → RY(org) + X^-(org) and the rapidly established liquid ion-exchange equilibria Y^-(aq) + Q^+X^-(org) ($K_{Y/X}^{sel}$) ⇌ X^-(aq) + Q^+Y^-(org). It is shown that the kinetic behavior is determined by $K_{Y/X}^{sel}$: $K_{Y/X}^{sel} < 1$ leads to "catalyst poisoning" and no simple rate law; $K_{Y/X}^{sel} = 1$ gives standard second-order behavior; $K_{Y/X}^{sel} > 1$ often leads to pseudo-first-order behavior. The efficiency of PTC, measured by the quotient of the observed rate constant and an intrinsic rate constant for the reaction conducted homogeneously in an appropriate solvent, k_{obsd}/k_{int}, is separated into two factors. The *physical* factor results from the inhomogeneous distribution of solutes and depends upon the concentrations of Y^-, X^-, catalytic (Q^+), and inert (M^+) cations, the volume fraction of the organic phase, and $K_{Y/X}^{sel}$ (and consequently the identity of solvent, Q^+, Y^-, and X^-). The *chemical* factor is determined primarily by ion-association and -solvation effects on Y^- in the organic phase and thus depends on identity of solvent, Y^-, and Q^+ and the ionic concentrations. Analytical expressions for the physical efficiency are derived for three cases: I, no X^- present initially; II, X^- present but $K_{Y/X}^{sel} = 1$; III, X^- present and $K_{Y/X}^{sel} \neq 1$. A collection of values of $K_{Y/X}^{sel}$ for anions of interest is presented for rough quantitative prediction of rate laws and efficiencies. The effects of PTC on rate and equilibrium in reversible second-order systems is also examined. When nucleophile Y^- is generated in situ from YH + OH^- the rapid distribution equilibria involve four species (YH, Y^-, OH^-, X^-) in two phases, but the rate law can still be treated numerically; the conditions for simple second-order kinetic behavior are determined.

Phase-transfer catalysis (PTC) increases the rate of reactions between nonelectrolyte substrates located in organic phases and ionic reagents located in a contacting aqueous phase.[2] The catalytic agents are salts of large organic ions. The reaction rates observed for a given reaction in these systems are determined in part by the chemical factors familiar in homogeneous media: an intrinsic rate modified by ion-solvation and ion-association forces. But in part the observed rates are governed by a more physical factor—the heterogeneity of the system and the distribution of the ions between the phases. This article investigates the nature of this distribution and analyzes the dependence of the catalytic efficiency upon it.

We limit consideration to second-order reactions and illustrate these, with little loss in generality, by the S_N2 reaction of substrate R-X with nucleophile Y^-. We identify the organic phase as (org), the aqueous phase as (aq), the inorganic counterion of reactant Y^- and product X^- as M^+, and the catalytic organic cation (most often a quaternary ammonium cation) as Q^+. The overall reaction is then

$$RX(org) + Y^-(aq) + M^+(aq) \xrightarrow{k_{obsd}} RY(org) + X^-(aq) + M^+(aq) \quad (1)$$

Phase-Transfer Catalysis as Liquid Ion-Exchange Catalysis. Three basic mechanisms[3] for PTC are shown below. Model A is a literal interpretation of the diagram first offered by Starks.[2,5] Model B is A with a different aqueous-phase reference state. Model C is that written in Starks's second paper.[6] Each model's equations sum to the overall reaction, eq. 1. Models A and B maintain the electroneutrality of the phases by anion-plus-cation transport (Figure 1a), model C by anion vs. anion transport (Figure 1b).

Model A

$t_{1/2}$, s

$$Q^+Y^-(org) + RX(org) \xrightarrow{k_2} RY(org) + Q^+X^-(org) \quad (2a)$$

$$\sim 10 \qquad Q^+X^-(org) \xrightarrow{k_3} Q^+X^-(aq) \quad (3a)$$

$$\sim 10^{-8} \qquad Q^+X^-(aq) + Y^-(aq) \xrightarrow{k_4} Q^+Y^-(aq) + X^-(aq) \quad (4a)$$

$$\sim 10 \qquad Q^+Y^-(aq) \xrightarrow{k_5} Q^+Y^-(org) \quad (5a)$$

Model B

$t_{1/2}$, s

$$Q^+Y^-(org) + RX(org) \xrightarrow{k_2} RY(org) + Q^+X^-(org) \quad (2b)$$

$$\sim 10 \qquad Q^+X^-(org) \overset{1/E_{QX}}{\rightleftharpoons} Q^+(aq) + X^-(aq) \quad (3b)$$

$$\sim 10 \qquad Y^-(aq) + Q^+(aq) \overset{E_{QY}}{\rightleftharpoons} Q^+Y^-(org) \quad (4b)$$